GROOVED TERRAIN FORMATION ON GANYMEDE DRIVEN BY MOBILE LID CONVECTION.

Amy C. Barr, Department of Geological Sciences, Brown University, Providence, RI 02910; amy_barr@brown.edu.

Background: Roughly two-thirds of Ganymede's surface is covered with bright lanes of grooved terrain. The terrain is thought to form during an epoch of increased orbital eccentricity, tidal heating, and diurnal tidal stress associated with Ganymede's capture into a Laplace-like resonance [1,2]. The terrain has morphological qualities consistent with a driving force that operated globally, but was capable of producing zones of intense local deformation [3]. Solid-state convection was proposed as a driving force [3], but convective stresses were thought to be too low to drive lithospheric deformation [4]. Here, I reevaluate the role of convection in grooved terrain formation in the context of new ideas about the interaction between convection and resurfacing based on observations of the south polar terrain of Enceladus [5-11].

Motivation: Prior studies assume that the heat flux from Ganymede during a resonance passage, F_{tidal}, was larger than the maximum heat flux that could be carried by convection. The ice shell was assumed to thin during resonance passage, stopping convection. Grooved terrain would form in response to lithospheric stresses from ice shell melting and freezing [2]. The estimated heat flux (F_{tidal}) for nominal values of the degree-2 Love number k_2, quality factor Q, and orbital eccentricity e, F_{conv}~40 mW m^{-2} (k_2/0.1) (100/Q) (e/0.04)^2 [2]. The maximum heat flux delivered by vigorous stagnant-lid convection (F_{conv}) is controlled by the rheology of ice [7], and for parameters appropriate for Ganymede, F_{conv}~50 mW m^{-2} (η_i/10^{14} Pa s)$^{-1/3}$ (where η_i is the viscosity in the warm convecting sublayer). For reasonable parameters, F_{conv}~F_{tidal}, suggesting that the ice shell could remain thick and convecting during resonance passage.

The inferred conditions for grooved terrain formation are not dissimilar from the heat flow and deformation rates inferred for the active south polar terrain [e.g., 7, 11] and ancient tectonic structures on Enceladus [12]. The characteristic double-wavelength structure of grooved terrain requires a near-surface gradient >10 to 30 K km^{-1}, and strain rates between 10^{-15} and 10^{-13} s^{-1} [13,14]. Models of flexural uplift at the flanks of the terrain suggest heat flows ~ 100 mW m^{-2} [15]. Estimates of the maximum heat flux experienced by the undisturbed dark terrain range from 60 to 80 mW m^{-2} [16]. By comparison, the total power output for the Enceladus south polar terrain of 15.8 ± 3.1 GW [10], spread over its ~70,000 km^2 total area [6], corresponds to F~225 mW/m^2.

The high heat flows have led several to suggest that the SPT on Enceladus is a location where the ice shell has become weakened, permitting convective plumes to reach close to the surface [7,8]. Conditions that give convective heat flows comparable to those observed also predict near-surface deformation rates ~10^{-14} s^{-1} [7,8]. A similar style of convection may also resurface Europa [17].

In an ice shell with a low yield stress, the convective flow field is time-dependent [18]. Narrow episodes of intense surface deformation and high heat flow form periodically, and initiate subduction of the near-surface ice [18,8]. Here, I show that this style of convection, which is suggested to drive deformation in the south polar terrain on Enceladus, may also create conditions conducive to grooved terrain formation.

Methods: The effect of the finite yield stress of a planetary lithosphere in mimicked in CITCOM [19] using a rheology of form [18, 20-22, 17],

$$\begin{aligned} \eta &= \eta_{creep} \quad \text{for} \quad \tau_{creep} < \tau_{yield} \\ \eta &= \eta_{yield} \quad \text{for} \quad \tau_{creep} \geq \tau_{yield}, \end{aligned} \tag{1}$$

where η_{creep} is the temperature-dependent viscosity of ice, $\eta_{yield} = \tau_{yield} / \dot{\varepsilon}_{II}$, where $\dot{\varepsilon}_{II}$ is the second invariant of the strain rate tensor, and $\tau_{yield}=C_o+\mu\rho g z$ [23], with the yield stress at zero lithostatic pressure C_o, and coefficient of friction on faults μ. The vigor of convection is described by the Rayleigh number,

$$Ra_o = \frac{\rho g \alpha \Delta T D^3}{\kappa \eta_o}, \tag{2}$$

with ice shell thickness D, ice density ρ=1000 kg m^{-3}, and gravity g=1.42 m s^{-2}, thermal expansion α=10^{-4} K^{-1}, thermal diffusivity κ=10^{-6} m^2 s^{-1}, temperature difference between the surface (T_s=130 K) and base (T_b=260 K) of the ice shell $\Delta T=T_b-T_s$, surface viscosity η_o ($\eta_o=\eta_1\Delta\eta$), and basal viscosity η_1=10^{13} to 10^{15} Pa s. Viscosity depends on temperature as $\eta(T)=\eta_o\exp(-\gamma T)$, where $\gamma=\theta/\Delta T$ and $\theta=\ln(\Delta\eta)$ [cf., 24].

Ice is assumed to flow by diffusion creep, which occurs by volume diffusion at conditions appropriate for Ganymede's ice mantle [25,26]. Although non-Newtonian deformation mechanisms can accommodate strain in the stagnant lid [27], the yield stress limits the viscosity to such an extent that these deformation mechanisms are unimportant. Mobile lid behavior occurs if the yield stress of the cold surface ice is less than a critical value [24],

$$\tau_{y,cr} \approx 13 \left(\frac{\alpha \rho g}{\Delta T} \right) \left(\frac{R_G T_i^2}{Q^*} \right)^2 l_{hor} \approx 60\,\text{kPa} \left(\frac{D}{50\,\text{km}} \right) \tag{3}$$

with, activation energy Q^*=59.4 kJ mol^{-1} [28], gas constant R_G=8.314 J mol^{-1} K^{-1}, temperature in the convecting layer T_i and plume spacing l_{hor}~D.

Here, I consider a basally heated ice shell because the spatial distribution of heating in a tidally heated shell is not well-constrained. Because the viscosity of ice is strongly temperature-dependent, the mode of heating does not significantly affect the criteria for the onset of mobile-lid behavior [24].

To determine whether mobile lid convection can create conditions similar to those inferred for the formation of grooved terrain, I performed a series of convection simulations in a simple 1x1 geometry for a range of Ra_o, $\Delta\eta$, and values of C_o~$\tau_{y,cr}$. A successful case must have: (1) regions where the local heat flow F~100 to 200 mW m^{-2}; (2) high strain rates ~ 10^{-15} to 10^{-13} s^{-1} within the regions of high F; (3) F<60 mW m^{-2} outside active regions.

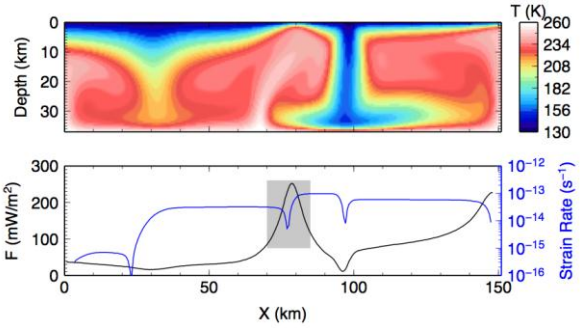

Figure 1. (top) Snapshot of the temperature field in a basally heated convecting ice shell on Ganymede with τ_{yield}~10 kPa, $\Delta\eta$=10^4, Ra_o=100, T_s=130 K, T_b=260 K. (bottom) Strain rate (blue) and local heat flux (black) as a function of distance. In a 15 km-wide zone near x=75 km (gray box), the local heat flow ~100-250 mW m^{-2} and strain rate ~10^{-14} to 10^{-13} s^{-1}, comparable to strain rates inferred for grooved terrain formation. Elsewhere, F<100 mW m^{-2}, consistent with the maximum heat flow experienced by the ancient dark terrain.

Results: The 1x1 calculations reveal that cases with low $\Delta\eta$~10^4, Ra_o<10^7 (corresponding to ~20-40 km-thick ice shells with η_1~10^{15} Pa s) and C_o<$\tau_{y,cr}$ satisfy criteria (1-3) above. Larger $\Delta\eta$ and Ra_o led to cases where the local heat flow during lithospheric spreading was much higher than inferred from the faulting style within groove lanes. Qualitatively, the successful cases represent a "mixture" of deformation styles, on the boundary between the stagnant- and mobile-lid regimes, with sluggish resurfacing.

Figure 1 illustrates a candidate successful case with $\Delta\eta$=10^4, Ra_o=10^6 (corresponding to D~37 km for Ganymede with η_1=10^{15} Pa s), and C_o~10 kPa simulated in a 4x1 box geometry to examine the convection pattern as it varies over time. Here, the plume in the center of the box overcomes the lithospheric yield strength. The active zone has F~220 mW m^{-2} and strain rates of 10^{-14} to 10^{-13} s^{-1} within a zone ~15 km wide (gray box). The local heat flow outside the active zone (x<70 km) remains below 100 mW m^{-2}. Lithospheric recycling occurs only within narrow zones confined between the plumes, rather than total lid recycling observed in higher $\Delta\eta$ and Ra_o cases.

Discussion: A style of convection inferred to form the south polar terrain on Enceladus can possibly form grooved terrain on Ganymede. During Ganymede's epoch of high eccentricity, it may be possible to form grooved terrain atop a convecting ice shell weakened by tidal stresses (to weaken the ice and give low C_o) and possibly heated at shallow depths [29] (to decrease the effective $\Delta\eta$). In addition, tidal stresses on Ganymede during this time may be sufficient to create zones of weakness that can be exploited by convection to form the terrain.

Acknowledgements: This work is supported by NASA PG&G NNX09AD94G.

References: [1] Showman, A. P., and R. Malhotra, *Icarus*, 127, 93–111, 1997; [2] Showman, A. P., D. J. Stevenson, and R. Malhotra, *Icarus*, 129, 367–383, 1997;[3] Shoemaker, E. M., B. K. Lucchitta, D. E. Wilhelms, J. B. Plescia, and S. W. Squyres, *Satellites of Jupiter*, pp. 435–520, 1982.[4] Squyres,; S. W. and S. K. Croft, in *Satellites*, pp. 293-341, 1986;[5] Spencer, J. R. et al., *Science* 311, 1401-1405, 2006; [6] Porco, C. C., et al., *Science* 311, 1391-1401,2006; [7] Barr, A. C., *JGR* 113 E07009, doi:10.1029/2008JE03114, 2008; [8]O'Neill, C. and F. Nimmo, *Nat. Geosci.* 3, 88-91, 2010; [9] Spencer, J. R. et al., in *Saturn from Cassini-Huygens*, pp. 683-724, 2009; [10] Howett, C. J. A, J. R. Spencer, J. Pearl, M. Segura, *JGR* 116, E03003, doi:10.1029/ 2010JE003718, 2011; [11] Barr, A. C. and L. J. Preuss, *Icarus*, 208, 499-503, 2010; [12] Bland, M. T., R. A. Beyer, A. P. Showman, *Icarus*, 192, 92-105, 2007; [13] Bland, M. T. and A. P. Showman, *Icarus*, 189, 439–456, 2007; [14] Bland, M. T., W. B. McKinnon, A. P. Showman, *Icarus* 210, 396-410, 2010; [15] Nimmo, F., R. T. Pappalardo, and B. Giese, *GRL* 29, 62-1, 1158, doi:10.1029/2001GL013976, 2002; [16] Nimmo, F. and R. T. Pappalardo, *GRL* 31, L19701, doi:10.1029/2004GL020763, 2004; [17] Showman, A. P. and L. Han, *Icarus* 177, 425-437, 2005; [18] Moresi, L.-N. and V. S. Solomatov, *Geophys. J. Int.* 133, 669-682, 1998; [19] Moresi, L.-N. and V. S. Solomatov, *Physics of Fluids*, 7, 2154-2162, 1995; [20] Trompert, R. and U. Hansen, *Nature* 395, 686-689,1998; [21] Tackley, P. J., *EPSL* 157, 9-22, 1998; [22] Tackley, P. J., 2000GC000036, *Geophys. Geochem. Geosyst.*, 1, 2000; [23] Byerlee, J., *J. Geophys. Res.*, 73, 4741–4750, 1968; [24] Solomatov, V. S., *JGR* 109, B01412, doi: 10.1029/2003JB002628, 2004; [25] McKinnon, W. B., *Icarus*, 183, 435–450, 2006; [26] Barr, A. C., and W. B. McKinnon, *J. Geophys. Res.*, 112, E02012, doi: 10.1029/2006JE002781, 2007; [27] Barr, A. C. and D. E. Stillman, *GRL* 38, L06203, doi: 10.1029/2010GL046616, 2011; [28] Goldsby, D. L., and D. L. Kohlstedt, *J. Geophys. Res.*, 106, 11,017–11,030, 2001; [29] Roberts, J. H. and F. Nimmo, *GRL* 35, L09201, doi: 10.1029/2008GL033725, 2008.